JOURNAL OF MATERIALS SCIENCE 11 (1976) 1354–1361

Generalized fracture mechanics

Part 2 *Materials subject to general yielding*

E. H. ANDREWS, E. W. BILLINGTON*
Department of Materials, Queen Mary College, Mile End Road, London, UK

The application of generalized fracture mechanics to ductile materials is considered. The deformations leading to crack propagation in SEN specimens of a copper-beryllium alloy in two conditions were established experimentally and can be described in terms of the generalized theory. In particular, it was possible to define and measure a surface work for fracture propagation in specimens subject to general yielding. The values of surface work obtained were 7.5×10^8 mJ m^{-2} for the alloy in a low yield stress (235 MPa) condition and 1.2×10^8 mJ m^{-2} for the high yield-stress (725 MPa) condition.

1. Introduction

Several methods, none of them altogether satisfactory, exist for the mechanical analysis of fracture in materials that undergo plastic yielding. They include crack opening displacement methods [1–3] and Rice's J contour integral [4–6] as discussed in a recent review by Turner [7] on yielding fracture mechanics. In both cases the fracture event is characterized by a critical value of the parameter concerned (δ_c or J_c) which, hopefully, is more or less independent of the shape, size, crack length and method of loading of the body under test.

In Part 1 [8] a generalized theory of fracture mechanics was outlined which potentially provides an additional approach to yielding fracture mechanics. In this theory the energy-density distribution throughout a specimen containing a crack is treated as an unknown function of the appropriate variables, and the changes in local energy-density caused by crack propagation are integrated over the entire stress field to give the net energy available for crack propagation.

In linear elastic media, of course, this method simply repeats the classical work of Griffith. The use of an unknown function for the energy-density however, relaxes the requirements of linearity and infinitesimal strain, so that an energy release rate $(-\mathrm{d}\mathfrak{E}/\mathrm{d}A)$ can still be defined when non-linear and finite elastic deformations occur in any part of the stress field. This provision then yields results compatible with the results of Rivlin and Thomas, employed so successfully to analyse the tearing of rubberlike materials [9]. It also makes the theory essentially equivalent to the J-integral theory for non-linear elastic materials, since it can be shown that [10]

$$J = -\mathrm{d}\mathfrak{E}/\mathrm{d}A \qquad (1)$$

so that

$$J_{IC} \equiv \mathcal{T} \qquad (2)$$

where $\mathfrak{E}$ is the total input energy of the system, A the crack area and $\mathcal{T}$ is the symbol employed in Part 1 for the critical energy release rate for crack propagation.

The generalized theory, however, goes further to consider explicitly the energy losses occurring in elements which unload as the crack begins to propagate. Under these circumstances, of course, energy-density is an input, and not a potential, energy whilst $(-\mathrm{d}\mathfrak{E}/\mathrm{d}A)$ becomes an apparent energy release rate. In these respects, the theory proposed in Part 1 appears to be unique and, as a direct consequence, it is possible not only to evaluate parameters such as $(-\mathrm{d}\mathfrak{E}/\mathrm{d}A)$ or J in terms of accessible quantities (like stress and linear dimensions) but also to provide a theoretical expression for the critical values $\mathcal{T}$ or J_c of such parameters. This is the most important new

* On secondment from RARDE (Ministry of Defence) Fort Halstead, Sevenoakes, Kent.

feature of the theory proposed in Part 1. Specifically,

$$\mathcal{J} = \mathcal{J}_0 \Phi(c, T, \epsilon_0) \tag{3}$$

$$\Phi = \left\{ \frac{\sum g(x, y, \epsilon_0)\, \delta x \delta y}{\sum g(x, y, \epsilon_0)\, \delta x \delta y - \sum_{\mathrm{PU}} \beta g(x, y, \epsilon_0)\, \delta x \delta y} \right\} \tag{4}$$

where: $\mathcal{J} \equiv J_{\mathrm{IC}}$ is the apparent surface work of fracture, Φ is the newly defined "loss function", g is the derivative with respect to x and y of the input energy density distribution function, x, y are the reduced (dimensionless) cartesian co-ordinates, and β is the fractional energy loss of an element subject to unloading. PU indicates summation only over unloading elements, and $\mathcal{J}_0$ is the actual energy required to break unit area of interatomic bonds across the fracture plane (the surface energy of the solid on one definition). Equation 3 has been highly successful in explaining certain adhesive failure phenomena [11, 12], whilst recent work on elastomers [13] has shown that Φ can be evaluated from the strain field around a crack, and the appropriate hysteresis data, to give excellent agreement with measured $(\mathcal{J}/\mathcal{J}_0)$ ratios (Equation 3).

The purpose of this paper is to report preliminary work on metal specimens which deform plastically before the onset of crack propagation. Any attempt to validate the generalized theory for a given class of materials must contain two stages. The first is to validate the equation expressing the apparent energy release rate $(-\mathrm{d}\mathcal{E}/\mathrm{d}A)$ in terms of accessible quantities, whilst the second is to explore the truth of Equation 3. The first step is by no means trivial and most of this paper is devoted to it.

For the case of either a centre crack in an infinite sheet under uniaxial tensile load, or the corresponding "half-plane" which constitutes an edge crack in a semi-infinite sheet, the appropriate equation is [8],

$$(-\mathrm{d}\mathcal{E}/\mathrm{d}A) = k_1(\epsilon_0)\, c W_0 \tag{5}$$

where k_1 is a function only of the strain-at-infinity ϵ_0 (or equivalently, of W_0), c is the crack length and W_0 is the input energy density at infinity. For finite specimens k_1 becomes a function of the specimen dimensions and ϵ_0, W_0 are the appropriate quantities at points remote from the crack.

The main purpose of this paper is to show that $(-\mathrm{d}\mathcal{E}/\mathrm{d}A)$ for an elastic-plastic material can indeed be presented by Equation 5; additionally, the function $k_1(\epsilon_0)$ is evaluated and the critical value, $\mathcal{J}$, of $(-\mathrm{d}\mathcal{E}/\mathrm{d}A)$ is shown to be constant under most, but not all, of the circumstances studied.

The experimental results are consistent with the idea that $\mathcal{J}$ has two regimes of constancy with a rapid transition between the two. Regime I applies to a small, elastically contained plastic zone and regime II to a plastic zone which interacts with the boundaries of the specimen. In a future paper we hope to demonstrate that just such a result can be inferred from Equations 3 and 4 using a simplified model of the plastic zone to evaluate Σ and thence Φ.

2. Definition of $k_1(\epsilon_0)$

In the previous paper [8] some ambiguity attaches to the definition of the energy change associated with unit area of crack propagation in an elastic medium, i.e. the quantity $-(\mathrm{d}\mathcal{E}/\mathrm{d}A)$ where $\mathcal{E}$ is the total energy and A the crack area. This ambiguity in turn affects the definition of $k_1(\epsilon_0)$, though not the validity of Equation 5. Although $k_1(\epsilon_0)$ is treated as an empirical quantity in this paper it is appropriate to resolve the matter at this point.

Consider the load–deformation curves, in tension, of identical sheets of an elastic, but non-linear material containing centre or edge cracks of different lengths (oriented perpendicular to the loading direction). A series of such curves is shown in Fig. 1 including the curve for $c = 0$, i.e. a sheet without a crack.

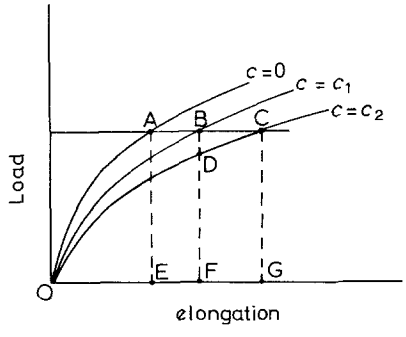

Figure 1 Load–deflection curves for SEN specimens containing cracks of different lengths (schematic).

Propagation of the crack from a length $2c_1$ to a length $2c_2$ at constant load (and thus at constant

ϵ_0, W_0) involves doing work on the specimen. This work being given by the area BCGF. The total elastic energy of the specimen, however, increases by the net amount $\Delta\mathfrak{E}$ such that,

$$[\Delta\mathfrak{E}/\Delta A]_{\epsilon_0} = (\text{BCGF} - \text{OBC})/4h(c_2 - c_1) \quad (6)$$

where h is the sheet thickness. Alternatively, if crack propagation occurs at constant deflection (so that the applied forces do no work during propagation), the specimen suffers an energy loss equivalent to area OBD. Thus

$$[\Delta\mathfrak{E}/\Delta A]_{\delta} = -(\text{OBD})/4h(c_2 - c_1). \quad (7)$$

Since in the limit $c_2 \to c_1$, area OBD $\to$ area OBC, we have from simple geometry in Fig. 1

$$|\mathrm{d}\mathfrak{E}/\mathrm{d}A|_{\delta} = \frac{-p}{1-p} |\mathrm{d}\mathfrak{E}/\mathrm{d}A|_{\epsilon_0} \quad (8)$$

where $0 < p < 1$ and $p = 0.5$ if curves OB, OC are linear. In the general, non-linear case

$$p = p(\epsilon_0). \quad (9)$$

In Part 1 the surface work $\mathcal{T}$ was wrongly equated to the critical value of $-(\mathrm{d}\mathfrak{E}/\mathrm{d}A)_{\epsilon_0}$ whereas it is properly defined as the critical value of $-(\mathrm{d}\mathfrak{E}/\mathrm{d}A)_{\delta}$. We thus re-define $k_1(\epsilon_0)$ as $-p/(1-p)$ times the expression given in Part 1, namely

$$k_1(\epsilon_0) = \frac{-p}{1-p} g(x, y, \epsilon_0)\, \delta x \delta y \quad (10)$$

where, as before, $g = \{x\partial f/\partial x + y\partial f/\partial y\}$. Then, as before

$$-|\mathrm{d}\mathfrak{E}/\mathrm{d}A|_{\delta} = k_1(\epsilon_0)\, cW_0 \quad (11)$$

$$\mathcal{T} = k_1(\epsilon_0)\, cW_{0,\text{crit}}. \quad (12)$$

These results, of course, are derived on the assumption that the material is elastic. In dealing with inelastic materials, as discussed in Part 1, we retain Equation 12 as a definition of the surface work $\mathcal{T}$ which, however, is no longer identifiable as a critical "energy release rate" since $\mathfrak{E}$ contains inelastic work terms. Similarly, W_0 is no longer a stored energy density but simply an energy input density. Stated simply, $\mathcal{T}$, is a fictional quantity equal to the critical energy release rate that would have obtained if the material had been elastic.

This fiction is not, of course, limited to the theory described in Part 1; it is employed every time linear elastic fracture mechanics is applied to real materials. The main novelty of the generalized theory is its ability to relate the parameter $\mathcal{T}$ to the genuine elastic energy release which actually drives the crack in inelastic solids.

3. Materials

The material chosen for the present study was a Cu–Be alloy of composition Cu 1.8 wt % Be 0.28 wt % Co. This alloy was selected because its deformation behaviour in tension exhibits a well-defined elastic-plastic character and because, by suitable conditioning treatments, the yield stress and plasticity can be varied, predictably, between wide limits. In this paper we report on one condition (designated A) which had been solution-treated for 1 h at 800° C and water-quenched, and a second condition (designated H) which had received a 50% cold-rolling treatment. Typical mechanical properties were as follows:

Temper	Tensile strength (MPa)	Yield strength (MPa) (strain)	VPN
A	500	235 (0.9%)	100
H	775	725 (2.9%)	220

Fig. 2 shows engineering-stress versus strain curves for the two conditions.

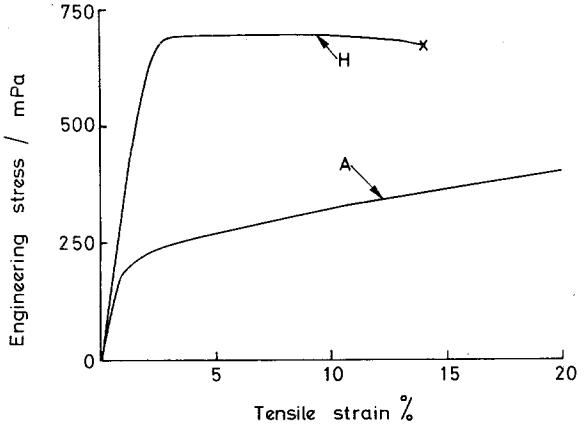

Figure 2 Actual stress–strain curves for conditions A and H. (x) indicates fracture.

4. Experimental

The initial purpose of the study was to determine the effect of blunt, single-edge cracks on the stress–strain and fracture properties of thin sheets of the materials. All testing was carried out on an Instron tensile testing machine.

For condition A three specimen widths were employed; narrow specimens 1.5 mm thick and

only 4.67 mm wide, intermediate specimens 1.0 mm thick and 20 mm wide, and wide specimens 1.0 mm thick and 42.0 mm wide. For the condition H only 1 mm thick and 42.0 mm wide specimens were tested. All specimens were machined with dumb-bell ends and had a gauge length of 100 mm.

Single edge cracks were machined into the specimens half way along their length and perpendicular to the tensile axis. In all cases the cracks were terminated by a drilled hole, diameters of 0.6, 1.0 and 1.25 mm being used in different experiments to eliminate crack-tip radius as an unknown variable. Although results obtained were insensitive to changes in radius within this range, it does not follow that this would be true of sharp cracks, and this must be kept in mind when evaluating the experimental data.

Crack length was varied as follows:

narrow specimens A	0, 0.66, 1.05, 1.40, 1.75 mm
intermediate specimens A	0, 2.1, 3.1, 3.6, 4.1, 4.6 mm
wide specimens A	0, 1, 2, 4, 6, 8 mm
wide specimens H	0, 1, 2, 4, 6, 8, 9, 12, 13 mm.

The specimens were subject to tensile loading at a cross-head speed of 1 mm min^{-1} and the tip of the crack watched continuously for signs of growth, using a travelling microscope. At the first sign of propagation, the "event marker" was used to indicate the corresponding point on the load–deformation curve.

5. Results and analysis

5.1. Evaluation of $k_1(\epsilon_0)$

Typical load–deformation curves for specimens containing cracks of different length are shown in Figs. 3 to 5. Fig. 3 shows typical data for material A and specimens of width 4.67 mm; Fig. 4, those for material A and specimens of width 42 mm, and Fig. 5, those for material H and width 42 mm. Each curve except those for $c = 0$, is terminated by a cross which represents the point at which the crack was observed to begin to propagate.

The purpose of the analysis of results is to evaluate from the above data the quantity $(-d\mathscr{E}/dA)_\delta$ for various W_0, c values in order to derive values for $k_1(\epsilon_0)$ or $k_1(W_0)$ (equivalent, since ϵ_0, W_0 are uniquely related) using the equation

$$-(d\mathscr{E}/dA)_\delta = k_1(\epsilon_0)\, cW_0. \qquad (5)$$

The left-hand side of this equation is obtained by first measuring the quantity $(\mathscr{E}_0 - \mathscr{E})$ in Fig. 1

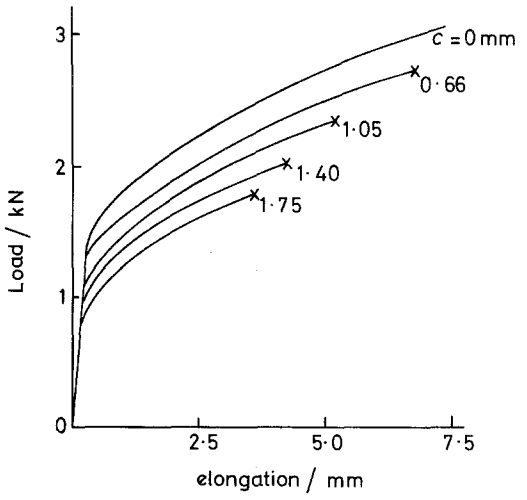

Figure 3 Actual load–deflection curves for narrow specimens of condition A containing single edge cracks of different lengths. (x) indicates fracture propagation.

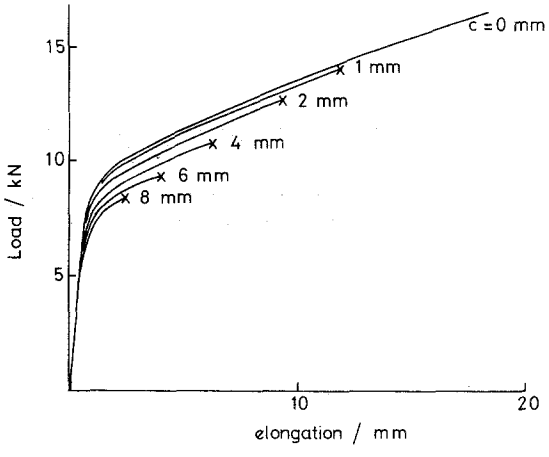

Figure 4 As Fig. 3 but for wide specimens of condition A.

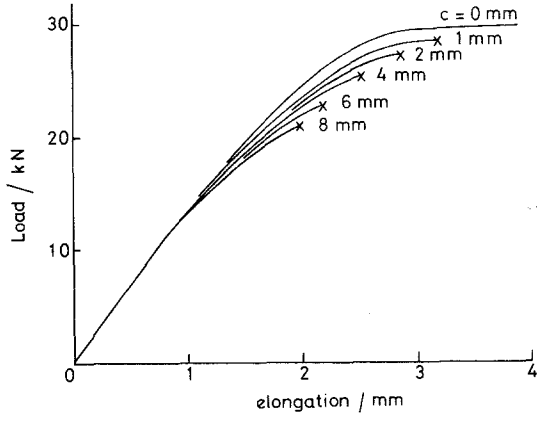

Figure 5 As Fig. 3 but for wide specimens of condition H.

given by the area

$$\text{OABF} - \text{OBF} = \text{OAB}$$

for a given W_0 and various c values. When plotted against c, the quantity $(\mathfrak{E}_0 - \mathfrak{E})$ gave a well-behaved square-law curve, the slope $(-\mathrm{d}\mathfrak{E}/\mathrm{d}c)_{W_0}$, of which was then obtained graphically and plotted, linearly, against c. These two curves are shown for a particular case, in Fig. 6. The fact that $(-\mathrm{d}\mathfrak{E}/\mathrm{d}A)$ {i.e. $(1/2h)(-\mathrm{d}\mathfrak{E}/\mathrm{d}c)$} plots linearly against c for constant W_0 is, of course, an important vindication of Equation 5 and demonstrates its validity even where the whole specimen is subject to plastic deformation.

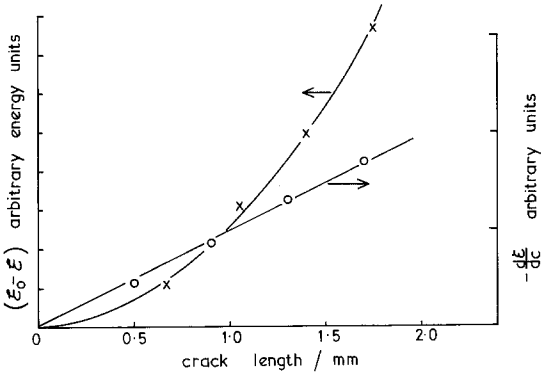

Figure 6 Evaluation of k_1 (see text).

The value of $k_1(W_0)$ is obtained from the slope S, of the linear plot in Fig. 6, by

$$k_1(W_0) = S/2hW_0 \qquad (13)$$

where h is the specimen thickness and W_0 is the input energy density for the uncracked specimen up to the strain ϵ_0.

The function $k_1(W_0)$ has the classical value of π for plane stress conditions as $W_0 \to 0$ i.e. for linear elastic material and infinitesimal strains [8]. Its behaviour for the present series of experiments is shown in Fig. 7 for the condition A.

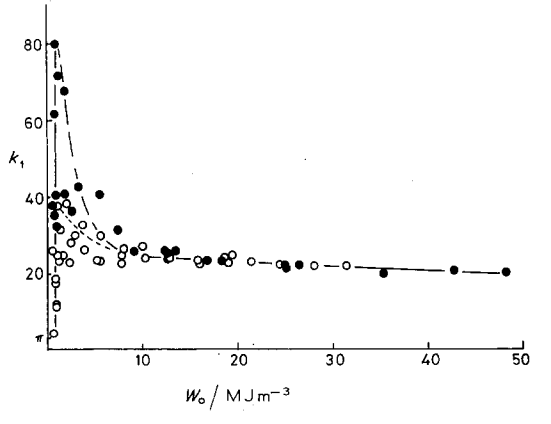

Figure 7 k_1 as a function of W_0 for condition A. •, narrow specimens; ○, wide specimens.

The results for k_1 exhibit an initial, very steep, rise from the value of π at $W_0 = 0$ to values in the range 20 to 40, for wide specimens and even higher, up to 80, for the narrow specimens: k_1 then falls again with increasing W_0 to a much more reproducible value of around 25 and continues to decrease slowly thereafter to 20 at the highest W_0 values used.

The "peak" area for k_1, over the range $0 < W_0 < 8\,\mathrm{MJ\,m^{-3}}$, corresponds to the onset of wholesale yielding in the specimen. In this range the k_1 values are badly scattered, but are noticeably higher for the narrow specimens. This almost certainly reflects the "hinging" mode of crack opening observed in these specimens, in which they undergo in-plane bending, causing the crack to gape. Clearly the plastic strain field is different in this case from that in the wider specimens where no hingeing can occur and this is reflected in the behaviour of k_1.

For the condition A, no crack growth was observed until the specimen had become fully plastic, so that fracture occurred only in the region $W_0 > 8\,\mathrm{MJ\,m^{-3}}$, i.e. where k_1 has settled down to a slowly varying value of 20 to 25.

A consequence of the dependence of k_1 on ϵ_0 (or W_0) alone is that, from Equation 5,

$$-\frac{1}{c}\left(\frac{\mathrm{d}\mathfrak{E}}{\mathrm{d}A}\right) = k_1(W_0)\,W_0 = f(W_0) \qquad (14)$$

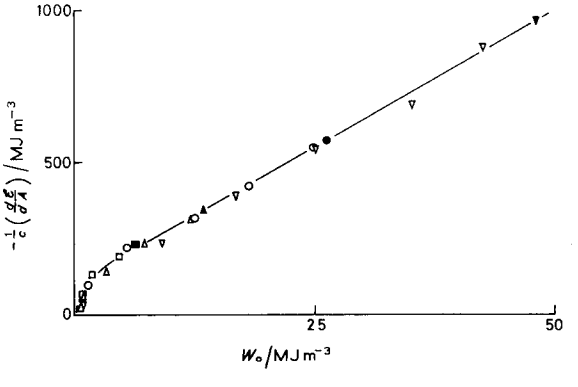

Figure 8 Data for narrow specimens of condition A showing validity of Equation 14. Filled symbols denote fracture point. ▽, $c = 0.66$ mm; ○, 1.05 mm; △, 1.40 mm; □, 1.75 mm.

i.e. the left-hand side should be a unique function of W_0, though only for linear, infinitesimal strain conditions will this be a linear relationship since only then is k_1 a constant. This behaviour is shown in Fig. 8 for the narrow specimens and Fig. 9 for the wide specimens, and these figures bear out fully the expectation of Equation 14. The effect of hinging is evident in the pronounced curvature of the plot for the narrow specimens.

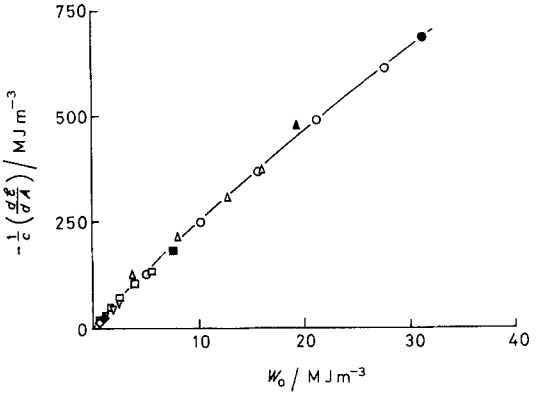

Figure 9 As Fig. 8 but for wide specimens of condition A. ○, $c = 1$ mm; △, 2 mm; □, 4 mm; ▽, 6 mm; ◇, 8 mm.

Analogous results for the cold-worked condition A are shown in Fig. 10. In this case a linear relation exists with a slope $k_1 = \pi$ up to the onset of gross yield i.e. the material obeys linear fracture mechanics. As the specimen stress–strain curve becomes non-linear, however, the curve turns sharply upwards. In view of the results for the softer alloy shown in Figs. 8 and 9, it is possible that the curve in Fig. 10 is, in fact, sigmoidal as shown by the broken line; i.e. k_1 rises from π to some transitory, high value, before settling down

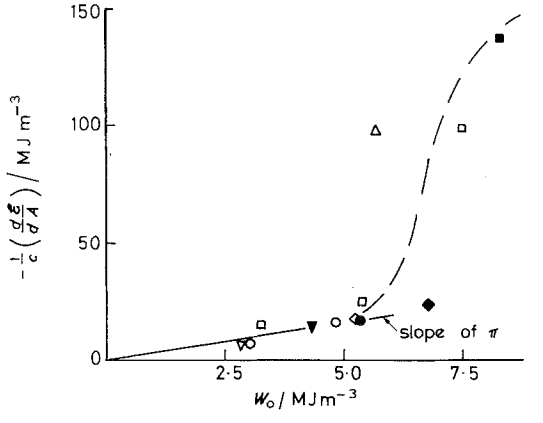

Figure 10 As Fig. 8 but for wide specimens of condition H. △, $c = 1$ mm; □, 2 mm; ◇, 4 mm; ○, 6 mm; ▽, 8 mm.

to a value of about 17 in the region of gross plasticity.

5.2. The surface work

The critical value of $(-d\mathcal{E}/dA)_\delta$ is, by definition, the surface work $\mathcal{T}$ and is given by

$$\mathcal{T} = k_1(\epsilon_0)\, cW_{0,\text{crit}}. \tag{8}$$

For brittle materials $\mathcal{T}$ is sensibly constant for a given solid under given conditions of rate and temperature and provided no plane stress-to-plane strain transition intrudes. The same is true of elastic but highly extensible materials like cross-linked elastomers.

It has not previously been possible to calculate surface work for solids which undergo substantial plastic deformation before fracture. Using Equation 12 however, we have

$$k_1\, W_{0,\text{crit}} = c^{-1} \tag{11}$$

and a plot of $k_1\, W_{0,\text{crit}}$ against c^{-1} should reveal whether or not a constant quantity $\mathcal{T}$ exists. Before making such a plot it is helpful to correct for the finite width of the specimen, since the above equations refer to infinite width. Rather than use established elastic corrections for finite width, whose application to plastic plates is hardly justifiable, we introduce a simple correction,

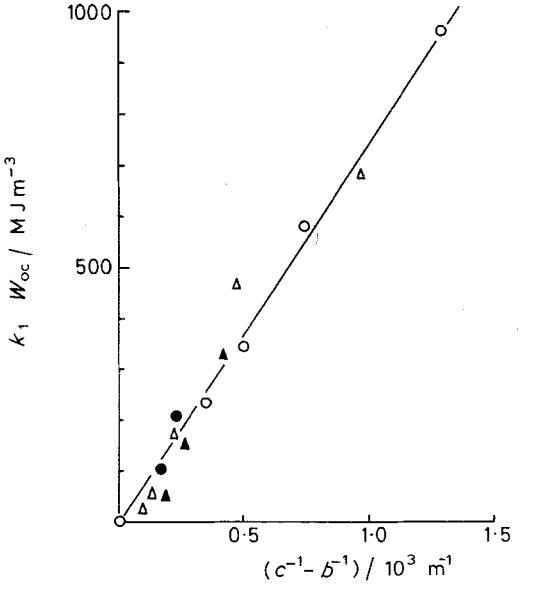

Figure 11 Plot of $k_1 W_{oc}$ against $(c^{-1} - b^{-1})$ for condition A having slope equal to the surface work. ○, narrow specimens, 1.0 mm tip radius; △, wide specimens, 1.0 mm tip radius; ▲, intermediate specimens, 1.25 mm tip radius; ●, intermediate specimens, 0.6 mm tip radius.

replacing c^{-1} by $(c^{-1} - b^{-1})$ where b is the specimen width. This satisfies the boundary conditions that $W_{0,\text{crit}} \to 0$ as $c \to b$ and that the correction itself tends to zero as $b \to \infty$.

The resulting plots for conditions A and H are shown in Figs. 11 and 12. Most data are available for alloy A where it will be seen that a linear relationship (i.e. constant $\mathcal{T}$) fits the data well and includes points for specimen widths b, ranging from 4.67 to 42 mm and for different crack tip radii. The value of $\mathcal{T}$ for this material derived from the best straight line in Fig. 11, is 7.5×10^8 mJ m^{-2}.

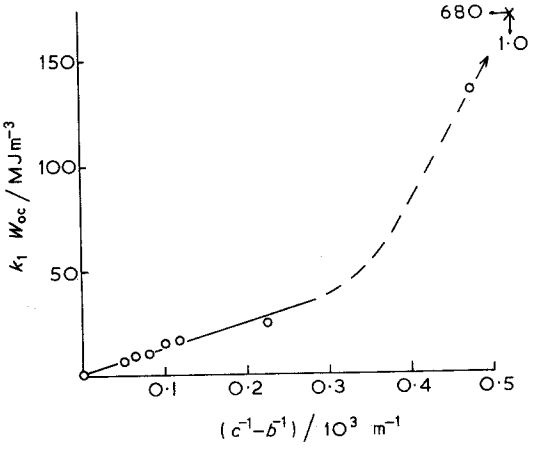

Figure 12 As Fig. 11 but for condition H (wide specimens). Point for 1 mm crack is off graph but its coordinates shown at X.

Fig. 12 reveals a more complicated situation for condition H. For cracks exceeding 2 mm in length the plot is linear giving a value for $\mathcal{T}$ of 1.2×10^8 mJ m^{-2}. For crack lengths of 2 and 1 mm however, the points lie well off the line, the apparent values of $\mathcal{T}$ increasing as follows:

Crack length (mm)	Apparent (mJ m^{-2})
> 2	1.2×10^8
2	2.7×10^8
1	6.7×10^8

Reference to Fig. 5 shows that specimens of condition H with crack lengths exceeding 2 mm, whilst displaying non-linear behaviour, do not exhibit gross yielding. Those with $c \leqslant 2$ mm show the attainment of extension at constant load. Specimens of condition A, in contrast, all fracture after gross yield and it is significant that the value obtained for condition A (7.5×10^8 mJ m^{-2}) is close to that obtained for the shortest crack length in condition H specimens, where gross yielding is also fully established.

These observations are consistent with the idea that, for a given material, the surface work $\mathcal{T}$ has two regimes of constancy. The first applies as long as the plastic zone is elastically contained i.e. does not intersect the boundaries of the specimen. As this containment fails, and the specimen thus begins to exhibit gross yielding, the surface work $\mathcal{T}$ increases rapidly until it achieves a new constancy (regime two) for the case of a fully plastic specimen as typified by condition A.

The transition between regimes one and two can be induced by changes in crack length, producing a notch-embrittlement effect. The same transition might, plausibly, be induced by changes in notch radius, temperature or rate of strain.

6. Conclusions

The use of generalized fracture mechanics makes it possible to analyse, rationally, the conditions for crack propagation in a fully ductile material in a manner analogous to the treatment of brittle solids by linear fracture mechanics. In particular it is possible to define and measure a unique "surface work" for crack propagation in a fully ductile alloy. The same analysis applied to a material which exhibits "notch embrittlement" gives a unique value for the brittle surface work, but a rising value as the crack length is diminished below a certain critical value. It is suggested that the dependence of surface work upon crack length in such cases might be used to quantify the phenomenon of notch embrittlement.

Acknowledgements

This work was carried out with the support of the Procurement Executive, Ministry of Defence.

References

1. F. M. BURDEKIN and D. E. W. STONE, *J. Strain Anal.* **1** (1966) 145.
2. A. A. WELLS, *J. Eng. Fract. Mech.* **1** (1968–70) 399.
3. T. KANAZAWA, S. MACHIDA, S. MOMOTO and Y. HAGIWARA, in "Fracture 1969" (Chapman and Hall, London, 1969) p. 1.
4. J. R. RICE, *J. Appl. Mech.* **35** (1968) 379.
5. J. R. RICE and G. F. ROSENGREN, *J. Mech. Phys. Solids* **16** (1968) 1.
6. F. MCCLINTOCK, "Fracture, An Advanced Treatise, 3", edited by Liebowitz (Academic Press, New York, 1971).

7. C. E. TURNER, *J. Strain Anal.* **10** (1975) 207.
8. E. H. ANDREWS, *J. Mater. Sci.* **9** (1974) 887.
9. *Idem*, "Fracture in Polymers" (Oliver and Boyd, Edinburgh, 1968) p. 138 *et seq.*
10. J. R. RICE, "Fracture, An Advanced Treatise, 2", edited by Liebowitz (Academic Press, New York, 1968).
11. E. H. ANDREWS and A. J. KINLOCH. *Proc. Roy. Soc. London* **A 332** (1973) 385.
12. *Idem, ibid* **A 332** (1973) 401.
13. Y. FUKAHORI, "Strength and Hysteresis of Rubber", Internal Report, Department of Materials, Queen Mary College, London (November 1975).

Received 23 July 1975 and accepted 6 January 1976.